2024 European Control Conference (ECC)
June 25-28, 2024. Stockholm, Sweden

Urban traffic congestion control: a DeePC change

Alessio Rimoldi*, Carlo Cenedese*, Alberto Padoan*, Florian Dörfler*, John Lygeros*

Abstract— **Urban traffic congestion remains a pressing challenge in our rapidly expanding cities, despite the abundance of available data and the efforts of policymakers. By leveraging behavioral system theory and data-driven control, this paper exploits the Data-enabled Predictive Control (DeePC) algorithm in the context of urban traffic control performed via dynamic traffic lights. To validate our approach, we consider a high-fidelity case study using the state-of-the-art simulation software package Simulation of Urban MObility (SUMO). Preliminary results indicate that DeePC outperforms existing approaches across various key metrics, including travel time and CO_2 emissions, demonstrating its potential for effective traffic management.**

I. Introduction

In the ever-growing urban landscapes of our times, the need for efficient and effective traffic congestion management systems has never been more pressing. Recent studies indicate that, on average, commuters in major American cities spend approximately 54 hours each year stuck in traffic jams [1]. The economic and environmental toll of traffic congestion is staggering [2]. As the world continues to urbanize, these figures are projected to increase significantly unless novel solutions for traffic congestion are developed.

In the era of digital transformation, data serves as a critical asset in this respect, revealing complex patterns of urban traffic and supporting data-informed decision-making [3]. In this context, the emergence of data-driven traffic control algorithms promises to revolutionize how we tackle the problem of urban traffic congestion [4]. With these premises, this paper addresses the urban traffic control problem using the DeePC algorithm [5].

Related work: In the past decades, the problem of urban traffic control has attracted the interest of many researchers. Early solutions focus on controlling traffic only in the proximity of traffic lights and intersections [6] and small traffic networks [7]. Over the years results have been developed for larger networks and have often considered as the main objective of the reduction the total system travel time or the emissions. The authors in [8] propose two different macroscopic models of urban traffic to design a Model Predictive Control (MPC) algorithm able to compute a structured network-wide traffic controller. Control strategies that focus particularly on reducing emissions can be found in [9]–[12] and references therein.

*Authors are with Automatic Control Laboratory, Department of Electrical Engineering and Information Technology, ETH Zürich, Physikstrasse 3 8092 Zürich, Switzerland {ccenedese,apadoan,fdorfler,jlygeros}@ethz.ch.

Research is supported by NCCR Automation and funded by the Swiss National Science Foundation (grant number 180545).

Due to the unprecedented data collection, storage, and computation capabilities, there has been a resurgence of interest in the control community in "direct" control approaches (see, e.g., the recent survey [13]). Leveraging behavioral system theory [14], these approaches infer optimal decisions directly from data. A particularly successful direct data-driven algorithm is DeePC [5], which has been applied in a wide array of practical case studies [5], [15], [16]. DeePC has been applied in the context of traffic control, e.g., to solve control problems related to the coordination of Connected Autonomous Vehicles (CAVs) [17], to vehicle rebalancing in mobility-on-demand systems [18]. However, to the best of our knowledge, DeePC has not been applied in the context of urban traffic congestion control due to the large-scale nature of the problem. Motivated and inspired by [19], [20], we propose a tractable formulation using an aggregate description of the urban traffic dynamics which mitigates these issues and the effect of unpredictable events.

Contributions: The main contributions of the paper are threefold. (i) We show that the DeePC algorithm, although fundamentally linear, excels in handling mildly nonlinear systems. Adopting the DeePC algorithm avoids the use of complex nonlinear models, but rather it generates optimal decisions directly from data. Instead, being able to generate control laws for traffic lights that do not directly regulate the flow among regions is extremely difficult via a traditional MPC based approach. (ii) We show that the building blocks necessary to deploy DeePC are simple to create after the partitioning of the city in homogenous regions, which should be performed only once as in [19]. This allows practitioners to bypass the identification of model parameters and, in case the infrastructure changes, new data can be collected and automatically updated in the algorithm. (iii) We show that the data-driven approach outperforms model-based approaches in terms of travel time and emission reduction via SUMO microscopic simulations.

The notation used in the paper is borrowed from [21], [22].

II. Preliminaries

1) Sequences and Hankel matrices: We consider finite and infinite sequences in $(\mathbb{R}^q)^{\mathbf{T}}$ and $(\mathbb{R}^q)^{\mathbb{N}}$, respectively. By a convenient abuse of notation, we often identify each finite sequence $w \in (\mathbb{R}^q)^{\mathbf{T}}$ with the corresponding vector $\mathrm{col}(w(1), \dots, w(T)) \in \mathbb{R}^{qT}$. We use the terms sequence and trajectory interchangeably.

The *Hankel matrix* of depth $L \in \mathbf{T}$ associated with the

finite sequence $w \in (\mathbb{R}^q)^{\mathbf{T}}$ is defined as

$$H_L(w) = \begin{bmatrix} w(1) & w(2) & \cdots & w(T-L+1) \\ w(2) & w(3) & \cdots & w(T-L+2) \\ \vdots & \vdots & \ddots & \vdots \\ w(L) & w(L+1) & \cdots & w(T) \end{bmatrix}.$$

2) Dynamical systems: A *dynamical system* (or, briefly, *system*) is a triple $\Sigma = (\mathbb{T}, \mathbb{W}, \mathcal{B})$ [14], where $\mathbb{T}$ is the *time set*, $\mathbb{W}$ is the *signal set*, and $\mathcal{B} \subseteq (\mathbb{W})^{\mathbb{T}}$ is the *behavior* of the system. We exclusively focus on *discrete-time* systems, with $\mathbb{T} = \mathbb{N}$ and $\mathbb{W} = \mathbb{R}^q$.

A system Σ is *linear* if the corresponding behavior $\mathcal{B}$ is a linear subspace, *time-invariant* if $\mathcal{B}$ is shift-invariant, *i.e.*, if $w \in \mathcal{B}$ implies $\sigma w \in \mathcal{B}$, and *complete* if $\mathcal{B}$ is closed in the topology of pointwise convergence [14, Proposition 4]. The model class of all complete Linear Time-Invariant (LTI) systems is denoted by $\mathcal{L}^q$. By a convenient abuse of notation, we write $\mathcal{B} \in \mathcal{L}^q$.

The structure of an LTI system is characterized by a set of integer invariants known as *structure indices* [14]. The most important ones are the *number of inputs* m, *number of outputs* p, the *lag* ℓ, and the *order* n, see, [14, Section 7] for definitions. Every finite-dimensional LTI system admits a minimal representation and can be described by the equations

$$\sigma x = Ax + Bu, \quad y = Cx + Du, \tag{1}$$

where $\begin{bmatrix} A & B \\ C & D \end{bmatrix} \in \mathbb{R}^{(n+p)\times(n+m)}$ and m, n, and p are the number of inputs, the order, and the number of outputs, respectively.

3) Data-driven representations of dynamical systems: Given a trajectory $w_{\mathrm{d}} \in \mathbb{R}^{qT}$ of a system $\mathcal{B} \in \mathcal{L}^q$, it is possible to derive a non-parametric representation of its finite-horizon behavior using raw data. We summarize a version of this principle known as the *fundamental lemma* [23].

Lemma 1: [24, Corollary 19] Consider a system $\mathcal{B} \in \mathcal{L}^q$ with lag $\ell \in \mathbb{N}$ and a trajectory of the system $w_{\mathrm{d}} \in \mathcal{B}|_{[1,T]}$. Assume $L > \ell$. Then $\mathcal{B}|_{[1,L]} = \operatorname{im} H_L(w_{\mathrm{d}})$ if and only if

$$\operatorname{rank} H_L(w_{\mathrm{d}}) = mL + n, \tag{2}$$

where n and m are the order and the number of inputs of the system, respectively.

Lemma 1 is a key result in data-driven control [13]. It characterizes all trajectories of given length of an LTI system in terms of the image of a Hankel matrix. This foundational principle can be adapted in various ways, see the recent survey [13]. Remarkably, non-parametric representations have found practical use in data-driven control even when dealing with *nonlinear* systems [22], [25].

The rank condition (2) is known as the *generalized persistency of excitation* condition [24]. Note that upper bounds on the structure indices of $\mathcal{B}$ are necessary to check this condition from data.

III. Methodology

A. Urban traffic: sensing and dynamics

The transportation network of a city is composed of a collection of roads, highways, intersections, and points of interest such as bus stops. As in [19], the city can be partitioned in $p \in \mathbb{N}$ regions leveraging the concept of Macroscopic Fundamental Diagram (MFD). Partitioning a city into regions can be achieved through diverse methods, among which is the snake algorithm [26]. A forthcoming publication will provide comprehensive insights into the application of this method for city partitioning. These regions are identified such that the aggregate drivers' behavior traveling through it is as homogeneous as possible. The set of all regions is denoted by $\mathbf{p} \coloneqq \{1, \cdots, p\}$. Modern cities can choose among different types of sensors to assess traffic conditions. Among these, the most common (and reliable) are *Eulerian* sensors, such as single-loop detectors [27]. They can measure the number of vehicles that cross them during a fixed period and the occupancy, that is, the fraction of time during the same period that the sensor detected a vehicle above it [28]. Similar data can also be retrieved from other types of sensors, such as *Lagrangian* (or mobile) sensors. This includes vehicles equipped with transponders and GPS traveling through the city. For simplicity, however, we consider only Eulerian sensors throughout the paper.

We denote the number of sensors in each region $i \in \mathbf{p}$ as $s_i \in \mathbb{N}$ and the set of all sensors in the region is $\mathbf{s}_i \coloneqq \{1, \cdots, s_i\}$. From each sensor $j \in \mathbf{s}_i$, we can attain, from the occupancy and number of vehicles, the traffic density $\rho_j(t)$ [veh/km] and flow $\phi_j(t)$ [veh/h] during the time interval indexed by $t \in \mathbb{N}$ of length $\Delta \in \mathbb{R}_+$. We denote the density and flows measured in region $i \in \mathbf{p}$ during t by

$$\boldsymbol{\rho}_i(t) \coloneqq \operatorname{col}((\rho_1(t)), \cdots, \rho_{s_i}(t))) \in \mathbb{R}^{s_i} \tag{3a}$$

$$\boldsymbol{\phi}_i(t) \coloneqq \operatorname{col}((\phi_1(t), \cdots, \phi_{s_i}(t))) \in \mathbb{R}^{s_i}. \tag{3b}$$

Similarly, the aggregate vectors of all densities and flows in the city during t are, respectively,

$$\boldsymbol{\rho}(t) \coloneqq \operatorname{col}((\boldsymbol{\rho}_i(t))_{i\in\mathbf{p}}) \in \mathbb{R}^s \tag{4a}$$

$$\boldsymbol{\phi}(t) \coloneqq \operatorname{col}((\boldsymbol{\phi}_i(t))_{i\in\mathbf{p}}) \in \mathbb{R}^s, \tag{4b}$$

where $s = \sum_{i\in\mathbf{p}} s_i$.

The evolution of traffic within the city depends on the number of commuters entering the system during every time interval within each region. We call this flow of vehicles *demand*. The flow of vehicles starting their trip in region $i \in \mathbf{p}$ at time t and aiming to end the trip in region $j \in \mathbf{p}$ is denoted by $d_{ij}(t)$ [veh/h], while $d_{ii}(t)$ [veh/h] is the *internal trip completion flow* [19], which describes the flow of vehicles whose final destination is region i. The aggregate vector of demands associated with region i is denoted by $\boldsymbol{d}_i(t) \coloneqq \operatorname{col}((d_{ij}(t))_{j\in\mathbf{p}}) \in \mathbb{R}^p$ while the vector of all the demands among all regions is $\boldsymbol{d}(t) \coloneqq \operatorname{col}((\boldsymbol{d}_i(t))_{i\in\mathbf{p}}) \in \mathbb{R}^{p^2}$. Hereafter, we consider the *nominal* value of $\boldsymbol{d}(t)$ as an exogenous and known quantity.

Policymakers throughout the years have designed a plethora of interventions to reduce urban traffic congestion [29]. Among dynamic policies is the installation of controllable traffic lights [30]. By strategically controlling the flow of vehicles traveling through an intersection, it is possible to indirectly influence $\boldsymbol{\phi}_i(t)$ and $\boldsymbol{\rho}_i(t)$ in each region. Given two regions $i, j \in \mathbf{p}$, if one (or multiple)

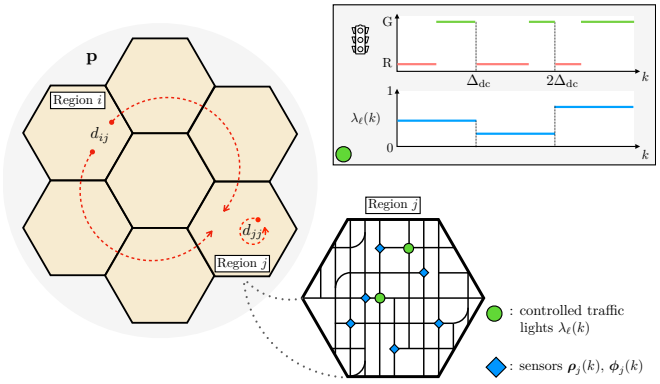

Fig. 1: The city is divided into p regions (the hexagons) based on their MFD and the demand $\boldsymbol{d}$ among them. The qualitative detail of how sensors $\mathbf{s}_j$ (blue diamonds) and traffic lights $\mathbf{l}$ (green circles) might be positioned within a region $j \in \mathbf{p}$. The top part illustrates how the control input λ_ℓ influences the duty cycle of a traffic light $\ell \in \mathbf{l}$.

intersection used by drivers to move from i to j allows for a smaller flow to pass through, then the vehicles will accumulate increasing the density in i and decreasing the flow from i to j. The flow of vehicles that can travel through a intersection can be controlled by varying the ratio between green time $\lambda(t)$ and duty cycle period $\Delta_{\text{dc}} \in \mathbb{N}$, see Fig. 1. Therefore, the control input $\lambda_\ell(t) \in [\underline{\lambda}_\ell, \overline{\lambda}_\ell] \subseteq [0,1]$ where $\lambda_\ell(t) = 1$ means that the traffic light is always green and $\lambda_\ell(t) = 0$ red for the whole duty cycle. The vector of all input associated with the l controlled traffic lights is denoted by $\boldsymbol{\lambda}(t) = \text{col}((\lambda_\ell(t))_{\ell \in \mathbf{l}})$, where $\mathbf{l} := \{1, \cdots, l\}$.

We model the nonlinear dynamics associated with the density evolution measured by the sensors as

$$\boldsymbol{\rho}(t+1) = f(\boldsymbol{\rho}(t), \boldsymbol{\lambda}(t), \boldsymbol{d}(t)), \tag{5}$$

where $f : \mathbb{R}^{s+l+p^2} \to \mathbb{R}^s$ is not known. In this preliminary study, we simplify the analysis by exclusively modelling the density dynamics. This choice mitigates the curse of dimensionality associated with the proposed data-driven approach. However, preliminary results suggest that considering the intrinsic link between flow and density evident in the MFDs may enhance performance. This will be elaborated upon in a future publication.

As discussed in [31], aggregating data from the sensor within a region helps reduce the variability and capture the macroscopic variation in density. An aggregating function has the role of mapping the sensors' measured densities to the associated region density. So, the *average* density of region i is attained as $\overline{\rho}_i(t) = h_i(\boldsymbol{\rho}_i(t))$, where $h_i : \mathbb{R}^{s_i} \to \mathbb{R}$ is the aggregating function of region $i \in \mathbf{p}$. Consequently, we define the complete aggregation function as $h : \mathbb{R}^s \to \mathbb{R}^p$

$$\overline{\boldsymbol{\rho}}(t) = h(\boldsymbol{\rho}(t)) := \text{col}\left((h_i(\boldsymbol{\rho}_i(t)))_{i \in \mathbf{p}}\right). \tag{6}$$

Using the density dynamics of the city regions in (5)–(6) and the definition in Section II, we now introduce the behavior $\mathcal{B}_{\text{c}}$ that describes the associated dynamical system

$$\mathcal{B}_{\text{c}} = \{(\boldsymbol{\lambda}, \boldsymbol{d}, \overline{\boldsymbol{\rho}}) \in \mathbb{R}^{m+p} \,:\, \exists \boldsymbol{\rho} \in \mathbb{R}^s \text{ s.t (5)–(6) hold}\}, \tag{7}$$

where $m = l + p^2$ and $u = (\boldsymbol{\lambda}, \boldsymbol{d}) \in \mathbb{R}^m$ is the input, divided in controllable and exogenous, and $\overline{\boldsymbol{\rho}}$ the output.

B. The DeePC algorithm

1) Setup and assumptions: Consider a (possibly unknown) LTI system $\mathcal{B} \in \mathcal{L}^{m+p}$, with m inputs and p outputs. Assume that data recorded offline from system $\mathcal{B}$ are available. Specifically, assume that an input sequence $u_{\text{d}} = \text{col}(u_{\text{d}}(1), \cdots, u_{\text{d}}(T)) \in \mathbb{R}^{mT}$ of given length $T \in \mathbb{N}$ is applied to the system $\mathcal{B}$ and that the corresponding output sequence is $y_{\text{d}} = \text{col}(y_{\text{d}}(1), \cdots, y_{\text{d}}(T)) \in \mathbb{R}^{pT}$. The subscript "d" is used to indicate that these are sequences of data samples collected offline. Finally, let $T_{\text{ini}} \in \mathbb{N}$ and $T_{\text{f}} \in \mathbb{N}$, with $T_{\text{ini}} + T_{\text{f}} \leq T$, and assume that the sequence $w_{\text{d}} \in \mathbb{R}^{(m+p)T}$, defined as $w_{\text{d}}(t) = \text{col}(u_{\text{d}}(t), y_{\text{d}}(t))$ for $t \in \mathbf{T}$, satisfies the generalized persistency of excitation condition (2), where $L = T_{\text{ini}} + T_{\text{f}}$ and n is the order (or an upper bound on the order) of the system.

2) Data organization: Next, we partition the input/output data into two parts which we call *past data* and *future data*. Formally, given the time horizons $T_{\text{ini}} \in \mathbb{N}$ and $T_{\text{f}} \in \mathbb{N}$ associated with the past data and the future data, we define

$$\begin{pmatrix} U_{\text{p}} \\ U_{\text{f}} \end{pmatrix} = H_{T_{\text{ini}}+T_{\text{f}}}(u_{\text{d}}), \quad \begin{pmatrix} Y_{\text{p}} \\ Y_{\text{f}} \end{pmatrix} = H_{T_{\text{ini}}+T_{\text{f}}}(y_{\text{d}}), \tag{8}$$

where $U_{\text{p}} \in \mathbb{R}^{(mT_{\text{ini}}) \times (T - T_{\text{ini}} + 1)}$ consists of the first T_{ini} block-rows of the matrix $H_{T_{\text{ini}}+T_{\text{f}}}(u_{\text{d}})$ and $U_{\text{f}} \in \mathbb{R}^{(mT_{\text{f}}) \times (T - T_{\text{f}} + 1)}$ consists of the last T_{f} block-rows of the matrix $H_{T_{\text{ini}}+T_{\text{f}}}(u_{\text{d}})$ (similarly for Y_{p} and Y_{f}), respectively. In the sequel, past data denoted by the subscript "p" is used to estimate the initial condition of the underlying state, whereas the future data denoted by the subscript "f" is used to predict the future trajectories.

3) State estimation and trajectory prediction: By the fundamental lemma, any trajectory of the finite-horizon behavior $\mathcal{B}|_{[1,T_{\text{ini}}+T_{\text{f}}]}$ can be constructed using the data collected offline. Under the assumptions of Lemma 1, a trajectory $\text{col}(u_{\text{ini}}, y_{\text{ini}}, u, y)$ belongs to $\mathcal{B}|_{[1,T_{\text{ini}}+T_{\text{f}}]}$ if and only if there exists $g \in \mathbb{R}^{T - T_{\text{ini}} - T_{\text{f}} + 1}$ such that

$$\begin{pmatrix} U_{\text{p}} \\ Y_{\text{p}} \\ U_{\text{f}} \\ Y_{\text{f}} \end{pmatrix} g = \begin{pmatrix} u_{\text{ini}} \\ y_{\text{ini}} \\ u \\ y \end{pmatrix}. \tag{9}$$

For $T_{\text{ini}} \geq \ell$, the lag of the system, the output y is uniquely determined [13]. Intuitively, the trajectory $\text{col}(u_{\text{ini}}, y_{\text{ini}})$ specifies the underlying initial state from which the trajectory $\text{col}(u, y)$ evolves. This allows one to predict future trajectories based on a given initial trajectory $\text{col}(u_{\text{ini}}, y_{\text{ini}}) \in \mathcal{B}|_{[1,T_{\text{ini}}]}$, and the precollected data in U_{p}, U_{f}, Y_{p}, and Y_{f}. Indeed, given an initial trajectory $\text{col}(u_{\text{ini}}, y_{\text{ini}}) \in \mathcal{B}|_{[1,T_{\text{ini}}]}$ of length $T_{\text{ini}} \geq \ell$ and a sequence of future inputs $u \in \mathbb{R}^{mT_{\text{f}}}$, the first three block equations of (9) can be solved for g. The sequence of future outputs is then given by $y = Y_{\text{f}} g$.

Conversely, given a desired reference output y an associated control input u can be calculated.

4) DeePC algorithm: Given the future time horizon $T_\mathrm{f} \in \mathbb{N}$, a reference trajectory for the output $\hat{y} = (\hat{y}_0, \hat{y}_1, \cdots) \in (\mathbb{R}^p)^{\mathbb{N}}$ and input $\hat{u} = (\hat{u}_0, \hat{u}_1, \cdots) \in (\mathbb{R}^m)^{\mathbb{N}}$, past input/output data $w_\mathrm{ini} = \mathrm{col}(u_\mathrm{ini}, y_\mathrm{ini}) \in \mathcal{B}|_{[1,T_\mathrm{ini}]}$, input constraint set $\mathcal{U} \subseteq \mathbb{R}^{mT_\mathrm{f}}$, output constraint set $\mathcal{Y} \subseteq \mathbb{R}^{pT_\mathrm{f}}$, output cost matrix $Q \in \mathbb{R}^{p\times p}$, control cost matrix $R \in \mathbb{R}^{m\times m}$, regularization function $\psi : \mathbb{R}^{T-T_\mathrm{ini}-T_\mathrm{f}+1} \to \mathbb{R}$, and parameter $\lambda_y \in \mathbb{R}$, the DeePC algorithm relies on the solution of the optimization problem:

$$\begin{aligned} \min_{u,y,g,\sigma_y} \; & \sum_{k=1}^{T_\mathrm{f}} \|y(k) - \hat{y}(t+k)\|_Q^2 + \|u(k) - \hat{u}(t+k)\|_R^2 \\ & + \psi(g) + \lambda_y \|\sigma_y\|_1 \\ \text{s.t.} \; & \begin{pmatrix} U_\mathrm{p} \\ Y_\mathrm{p} \\ U_\mathrm{f} \\ Y_\mathrm{f} \end{pmatrix} g = \begin{pmatrix} u_\mathrm{ini} \\ y_\mathrm{ini} \\ u \\ y \end{pmatrix} + \begin{pmatrix} 0 \\ \sigma_y \\ 0 \\ 0 \end{pmatrix}, \\ & u \in \mathcal{U},\; y \in \mathcal{Y}. \end{aligned} \tag{10}$$

We are now ready to present the DeePC algorithm.

Algorithm 1 DeePC

Input: Data trajectories $w_\mathrm{d} = \mathrm{col}(u_\mathrm{d}, y_\mathrm{d}) \in \mathbb{R}^{(m+p)T}$, most recent input/output measurements $w_\mathrm{ini} = \mathrm{col}(u_\mathrm{ini}, y_\mathrm{ini}) \in \mathbb{R}^{(m+p)T_\mathrm{ini}}$, a reference trajectories $\hat{y} = (\hat{y}_0, \hat{y}_1, \cdots) \in (\mathbb{R}^p)^{\mathbb{N}}$, $\hat{u} = (\hat{u}_0, \hat{u}_1, \cdots) \in (\mathbb{R}^m)^{\mathbb{N}}$, input constraint set $\mathcal{U} \subseteq \mathbb{R}^{mT_\mathrm{f}}$, output constraint set $\mathcal{Y} \subseteq \mathbb{R}^{pT_\mathrm{f}}$, output cost matrix $Q \in \mathbb{R}^{p\times p}$, control cost matrix $R \in \mathbb{R}^{m\times m}$, regularization function $\psi : \mathbb{R}^{T-T_\mathrm{ini}-T_\mathrm{f}+1} \to \mathbb{R}$ and parameter $\lambda_y \in \mathbb{R}$.

1: Solve (10) for $g^\star$.
2: Compute optimal input sequence $u^\star = U_\mathrm{f} g^\star$.
3: Apply optimal input sequence $(u_t, \cdots, u_{t+j-1}) = (u_1^\star, \cdots, u_j^\star)$ for some $j \le T_\mathrm{f}$.
4: Set t to $t+j$ and update u_ini and y_ini to the T_ini most recent input/output measurements.
5: Return to 1.

C. DeePC for urban traffic control

We are now ready to introduce DeePC for the dynamical system $\mathcal{B}_\mathrm{c}$ describing the evolution of urban traffic.

1) Behavioral representation and constraints: The data matrix in (9) can be constructed using historical data. For $t \in \mathbf{T}$ the collection of input and output data used are respectively defined as $u_\mathrm{d}(t) \coloneqq \mathrm{col}(\boldsymbol{\lambda}(t), \boldsymbol{d}(t))$, $y_\mathrm{d}(t) \coloneqq \mathrm{col}(\overline{\boldsymbol{\rho}}(t))$. Using these sequences, we can construct the matrices in (8) as discussed in Section III-B.2. The data are collected offline and thus can be chosen among many different traffic scenarios that excited the dynamical system $\mathcal{B}_\mathrm{c}$ in different ways capturing a wide variety of the behaviors of the system. To construct u_ini and y_ini for the current time interval $t \in \mathbb{N}$, we simply collect the previous T_ini values of the input and outputs, $u_\mathrm{ini} \coloneqq \mathrm{col}(\boldsymbol{\lambda}(t - T_\mathrm{ini}), \boldsymbol{d}(t - T_\mathrm{ini}), \cdots, \boldsymbol{\lambda}(t), \boldsymbol{d}(t))$, $y_\mathrm{ini} \coloneqq \mathrm{col}(\overline{\boldsymbol{\rho}}(t - T_\mathrm{ini}), \cdots, \overline{\boldsymbol{\rho}}(t))$.

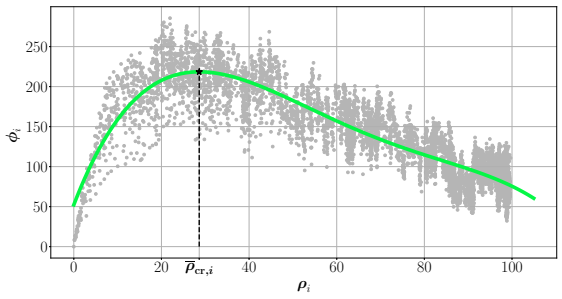

Fig. 2: The MFD for the region $i \in \mathbf{p}$, the historical measured data $\boldsymbol{\rho_i}, \boldsymbol{\phi_i} \in \mathbb{R}^{s_i}$ by the sensors $\mathbf{s_i}$ (light gray dots). The associated MFD for region $i \in \mathbf{p}$ (solid green line) displaying the relation between $\overline{\boldsymbol{\rho}}_i$ and $\overline{\boldsymbol{\phi}}_i$. The critical density $\overline{\boldsymbol{\rho}}_{\mathrm{cr},i}$ is the density maximizing the flow in the region $\overline{\boldsymbol{\phi}}_i$.

The control input has to satisfy the box constraints $\boldsymbol{\lambda}(k) \in [\underline{\boldsymbol{\lambda}}, \overline{\boldsymbol{\lambda}}] \subseteq \mathbb{R}^l$, where $\underline{\boldsymbol{\lambda}} = \mathrm{col}(\underline{\lambda}_1, \cdots, \underline{\lambda}_l)$ and $\overline{\boldsymbol{\lambda}}$ is defined similarly. Moreover, the green ratio cannot be changed during a duty cycle but only at the end of it, hence every Δ_dc time intervals of length Δ. This translates into the following linear constraint $M\boldsymbol{u} = \mathbf{0}$ on the variable $\boldsymbol{u}$ where $M \in \mathbb{R}^{mT_\mathrm{f}\times mT_\mathrm{f}}$ is used to impose for every $\ell \in \mathbf{l}$ and $k \le T_\mathrm{f}$ multiple of Δ_dc the constraint $\lambda_\ell(k+1) = \lambda_\ell(k+2) = \cdots = \lambda_\ell(k + \Delta_\mathrm{dc})$. On the contrary, the demand $\boldsymbol{d}$ is assumed to be a known, fixed exogenous input. Equal to the known demand $\overline{\boldsymbol{d}} = \mathrm{col}((\boldsymbol{d}(t), \cdots, \boldsymbol{d}(t + T_\mathrm{f}))) \in \mathbb{R}^{p^2 T_\mathrm{f}}$ over the prediction horizon, i.e., $Du = \overline{\boldsymbol{d}}$ with $D \in \mathbb{R}^{mT_\mathrm{f}\times p^2 T_\mathrm{f}}$ being a suitable matrix. Therefore, the set of constraints for the inputs over the whole prediction horizon reads as

$$\mathcal{U} = \left\{ u \in \left([\underline{\boldsymbol{\lambda}}, \overline{\boldsymbol{\lambda}}] \times \mathbb{R}_+^{p^2}\right)^{T_\mathrm{f}} \mid Mu = 0,\; Du = \overline{\boldsymbol{d}} \right\}. \tag{11}$$

The box constraints on the output ensure that the density in the region remains below the *grid-lock density* $\overline{\boldsymbol{\rho}}_{\max} \in \mathbb{R}_+^p$ (the density corresponding to zero flow), hence $y(t) \in [0, \overline{\boldsymbol{\rho}}_{\max}]$ and $\mathcal{Y} \coloneqq [0, \overline{\boldsymbol{\rho}}_{\max}]^{T_\mathrm{f}}$.

Finally, we apply to the system the first Δ_dc optimal input $\boldsymbol{\lambda}^\star$ values computed via Algorithm 1 and used to control the actuated traffic lights during the next duty-cycle.

2) Reference trajectory and cost function: Motivated and inspired by [20], we take advantage of the concept of MFD to estimate the optimal density for each region, $\hat{y}$ used in Algorithm 1. The concept of MFD formalizes the relation between the flow $\boldsymbol{\phi}_i$ and density $\boldsymbol{\rho}_i$ within a region $i \in \mathbf{p}$. As shown in Fig. 2, we can use the MFD to identify each region's $\overline{\rho}_{\mathrm{cr},i}$ that corresponds to the density ensuring the maximum flow within the region, thus $\overline{\boldsymbol{\rho}}_\mathrm{cr} = \mathrm{col}((\overline{\rho}_{\mathrm{cr},i})_{i\in\mathbf{p}})$ and $\hat{y} = (\overline{\boldsymbol{\rho}}_\mathrm{cr}, \overline{\boldsymbol{\rho}}_\mathrm{cr}, \cdots)$. In (10), we minimize the distance between the regions' densities and the critical ones. In a congested scenario, this implies maximizing the flow within the region.

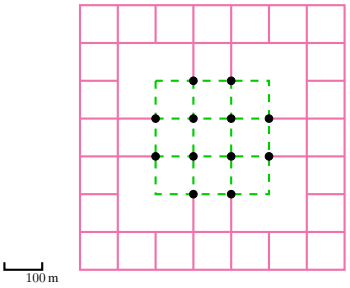

Fig. 3: The network is partitioned into the outer *region 0* (solid magenta line) and in *region 1* (dashed green line). Black dots represent the controlled traffic lights.

The reference value of the inputs $\hat{u}$ is composed of the one associated with $\boldsymbol{\lambda}$, and the one for the exogenous output. The former is constant and represents the ratio between green and red used by the traffic lights when no control is applied. The latter is exogenous and set equal to $\boldsymbol{d}$ according to (11).

In the cost function in (10), the matrices R and Q are chosen positive definite. Note that the components of $\|u - \hat{u}\|_R$ associated with $\boldsymbol{d}$ are always equal to zero due to the chosen reference and the constraints on u. Finally, the regularization term ψ is chosen as in [5].

IV. Simulations

In this section, we compare the DeePC algorithm against the MPC formulated in [32]. We study the behavior of DeePC and MPC in a congested and an uncongested scenario. The main difference between the two is the demand in the network. Both scenarios are modeled using the state-of-the-art simulation software package SUMO [33]. The emission model used in the simulations is HBEFA v2.1-based [34]. All simulations are conducted on a 3.6 GHz AMD Rizen 7 4000 Series processor.

We consider a lattice network whose topology is shown in Fig. 3. The network is composed of 208 roads (each one equipped with a sensor) connected by 64 intersections, of which 12 act as actuators. The duty cycle of the traffic lights has a duration of $\Delta_{\text{dc}} = 1.5$ [min]. All vehicles are assumed to be cars. The simulation spans one hour. Perimeter control requires the network to be partitioned into regions, composed of roads that are similar in terms of average density producing a low scattered MFD. Fig. 3 shows the partitioning used, where we define two regions *region 0* (solid magenta lines) and *region 1* (dashed green lines).

The demand in the network is directional, all trips generated move from *region 0* to *region 1*. This simulates the flow of vehicles traveling during the morning peak hours from the outskirts of a city to the city center, i.e., from region 0 to 1. The demand has a triangular shape, peaking at t =30 [min] with a base of length 13 [min]. The maximum flow is 180 [veh/h] in the uncongested setting and 1080 [veh/h] in the congested scenario. We compare the controllers also to the

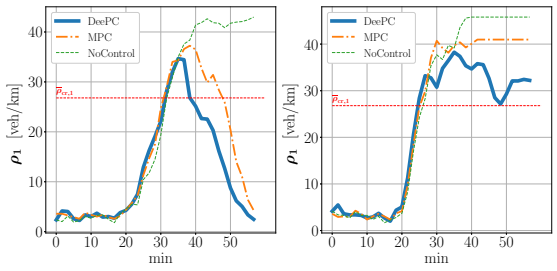

(a) Density in region 1

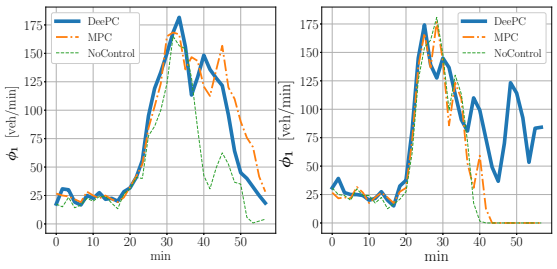

(b) Flow in region 1

Fig. 4: Density (a) and flow (b) in region 1 in uncongested (left column) and congested (right column) scenarios.

No Control baseline (No Control), hence a simulation where the actuators' input $\boldsymbol{\lambda}$ is constant and equal to the default ratio used by SUMO. The average travel time of No Control in the uncongested scenario is 9.3 [min] of which 6.7 [min] is waiting time due to traffic congestion. In the congested case, the average travel time rises to 20.6 [min] with 18.4 [min] of waiting time.

TABLE I: Performance and emissions of DeePC, MPC, and No Contol (NoC.) in uncongested and congested scenarios.

	Uncongested			Congested		
	DeePC	MPC	NoC.	DeePC	MPC	NoC.
TT (min)	**5.84**	6.56	9.33	**18.4**	20.6	20.6
WT (min)	**2.89**	3.51	6.74	**15.6**	18.4	18.4
CO (10^{-2}kg)	**3.9**	4.6	7.6	**16.8**	19.2	19.2
CO_2 (10^{-2}kg)	**95.8**	108	150	**289**	324	325
HC (10^{-4}kg)	**2.03**	2.38	3.84	**8.35**	9.50	9.54
PMx (10^{-4}kg)	**0.20**	0.23	0.34	**0.70**	0.79	0.79
NOx (10^{-4}kg)	**4.16**	4.69	6.68	**13.1**	14.7	14.8

TT: Average travel time, WT: Average waiting time.

Table I shows that DeePC outperforms No Control and MPC both in terms of average travel time and CO_2 emissions reduction. DeePC also decreases the average travel time in the uncongested case by 37.4% over No Control, compared with the 29.6% obtained by MPC. Fig.4a highlights that DeePC maintains the density closer $\overline{\rho}_{\text{cr}}$, which in turn maximizes the flow Fig. 4b leading to the lower travel time. By taking the average time saved and CO_2 emissions and multiplying them by the number of vehicles, we get the total travel time and CO_2 that have been saved, respectively 151 [h] and 1411 [kg] for DeePC. In the congested case,

DeePC reduces the travel time by 10,7%, while MPC does not perform significantly better than the No Control baseline. This is because DeePC prevents a gridlock state, as shown in Fig. 4b, and achieves substantially higher flows after $t = 40$ [min]. The total travel time and CO_2 emissions saved in this scenario by using the DeePC are 318 [h] and 3113 [kg].

We applied the proposed control scheme to the more complex microsimulation of the city of Zürich. The preliminary results attained are omitted due to space limitations and can be found in [35]. An in-depth analysis of this complex scenario will be the topic of future research.

V. Conclusion

As urban areas continue to expand, exacerbating traffic congestion and emissions, data-driven traffic management strategies offer effective solutions to reduce congestion and emissions. This paper has leveraged the data-driven control algorithm DeePC to address the urban traffic control problem. Our preliminary results, based on a case study using the high-fidelity SUMO simulation software, suggests the great promise of the data-driven approach exemplified by DeePC in outperforming existing methods, particularly in key metrics such as travel time and CO_2 emissions. Future research should explore the engineering relevance of this approach with a real-world case study.

References

[1] D. Schrank, B. Eisele, and T. Lomax. (2019) 2019 urban mobility report. Texas A&M Transportation Institute. [Online]. Available: https://mobility.tamu.edu/umr/

[2] Council and the European Parliament. (2019) Fit for 55 package. [Online]. Available: https://www.consilium.europa.eu/en/policies/green-deal/timeline-european-green-deal-and-fit-for-55/

[3] L. Atzori, A. Iera, and G. Morabito, "The internet of things: A survey," *Computer Networks*, vol. 54, no. 15, pp. 2787–2805, 2010.

[4] Y. Li, J. Hong, and L. Zhang, "Urban traffic signal control: A comprehensive review," *IEEE Transactions on Intelligent Transportation Systems*, vol. 21, no. 1, pp. 380–394, 2020.

[5] J. Coulson, J. Lygeros, and F. Dörfler, "Data-enabled predictive control: In the shallows of the DeePC," in *Proc. Eur. Control Conf.*, Naples, Italy, 2019, pp. 307–312.

[6] D. I. Robertson and R. D. Bretherton, "Optimizing networks of traffic signals in real time-the scoot method," *IEEE Transactions on vehicular technology*, vol. 40, no. 1, pp. 11–15, 1991.

[7] M. Papageorgiou, C. Diakaki, V. Dinopoulou, A. Kotsialos, and Y. Wang, "Review of road traffic control strategies," *Proceedings of the IEEE*, vol. 91, no. 12, pp. 2043–2067, 2003.

[8] S. Lin, B. De Schutter, Y. Xi, and H. Hellendoorn, "Efficient network-wide model-based predictive control for urban traffic networks," *Transportation Research Part C: Emerging Technologies*, vol. 24, pp. 122–140, 2012.

[9] ——, "Integrated urban traffic control for the reduction of travel delays and emissions," *IEEE Transactions on Intelligent Transportation Systems*, vol. 14, no. 4, pp. 1609–1619, 2013.

[10] C. Cenedese, P. Stokkink, N. Geroliminis, and J. Lygeros, "Incentive-based electric vehicle charging for managing bottleneck congestion," *European Journal of Control*, vol. 68, p. 100697, 2022.

[11] P. D. Grontas, C. Cenedese, M. Fochesato, G. Belgioioso, J. Lygeros, and F. Dörfler, "Designing optimal personalized incentive for traffic routing using big hype algorithm," *Proc. 62th Conf. Decision Control*, 2023.

[12] Q. Guo, L. Li, and X. J. Ban, "Urban traffic signal control with connected and automated vehicles: A survey," *Transportation research part C: emerging technologies*, vol. 101, pp. 313–334, 2019.

[13] I. Markovsky and F. Dörfler, "Behavioral systems theory in data-driven analysis, signal processing, and control," *Ann. Rev. Control*, vol. 52, pp. 42–64, 2021.

[14] J. C. Willems, "From time series to linear system—Part I. Finite dimensional linear time invariant systems," *Automatica*, vol. 22, no. 5, pp. 561–580, 1986.

[15] P. G. Carlet, A. Favato, S. Bolognani, and F. Dörfler, "Data-driven predictive current control for synchronous motor drives," in *IEEE Energy Conversion Congress and Exposition*, Detroit, MI, USA, 2020, pp. 5148–5154.

[16] L. Huang, J. Coulson, J. Lygeros, and F. Dörfler, "Data-enabled predictive control for grid-connected power converters," in *Proc. 58th Conf. Decision Control*, Naples, Italy, 2019, pp. 8130–8135.

[17] J. Wang, Y. Zheng, K. Li, and Q. Xu, "DeeP-LCC: data-enabled predictive leading cruise control in mixed traffic flow," *IEEE Transactions on Control Systems Technology*, 2023.

[18] P. Zhu, G. Ferrari-Trecate, and N. Geroliminis, "Data-enabled predictive control for empty vehicle rebalancing," in *European Control Conference*, 2023, pp. 1–6.

[19] I. I. Sirmatel and N. Geroliminis, "Economic model predictive control of large-scale urban road networks via perimeter control and regional route guidance," *IEEE Transactions on Intelligent Transportation Systems*, vol. 19, no. 4, pp. 1112–1121, 2018.

[20] N. Geroliminis, J. Haddad, and M. Ramezani, "Optimal perimeter control for two urban regions with macroscopic fundamental diagrams: A model predictive approach," *IEEE Transactions on Intelligent Transportation Systems*, vol. 14, no. 1, pp. 348–359, 2013.

[21] A. Padoan, J. Coulson, H. J. van Waarde, J. Lygeros, and F. Dörfler, "Behavioral uncertainty quantification for data-driven control," in *Proc. 61st Conf. Decision Control*, Cancun, Mexico, 2022, pp. 4726–4731.

[22] A. Padoan, F. Dörfler, and J. Lygeros, "Data-driven representations of conical, convex, and affine behaviors," in *Proc. 62nd Conf. Decision Control*, Singapore, 2023, pp. 596–601.

[23] J. C. Willems, P. Rapisarda, I. Markovsky, and B. L. M. De Moor, "A note on persistency of excitation," *Syst. Control Lett.*, vol. 54, no. 4, pp. 325–329, 2005.

[24] I. Markovsky and F. Dörfler, "Identifiability in the behavioral setting," *IEEE Trans. Autom. Control*, vol. 68, no. 3, pp. 1667–1677, 2023.

[25] J. Berberich, J. Köhler, M. A. Müller, and F. Allgöwer, "Linear tracking mpc for nonlinear systems — Part II: The data-driven case," *IEEE Transactions on Automatic Control*, vol. 67, no. 9, pp. 4406–4421, 2022.

[26] M. Saeedmanesh and N. Geroliminis, "Clustering of heterogeneous networks with directional flows based on "snake" similarities," *Transportation Research Part B: Methodological*, vol. 91, pp. 250–269, 2016.

[27] Z. Jia, C. Chen, B. Coifman, and P. Varaiya, "The PeMS algorithms for accurate, real-time estimates of g-factors and speeds from single-loop detectors," in *ITSC 2001. 2001 IEEE Intelligent Transportation Systems. Proceedings (Cat. No.01TH8585)*, 2001, pp. 536–541.

[28] C. G. Claudel and A. M. Bayen, "Guaranteed bounds for traffic flow parameters estimation using mixed lagrangian-eulerian sensing," in *2008 46th Annual Allerton Conference on Communication, Control, and Computing*, 2008, pp. 636–645.

[29] E. Elokda, C. Cenedese, K. Zhang, J. Lygeros, and F. Dörfler, "Carma: Fair and efficient bottleneck congestion management with karma," *arXiv preprint arXiv:2208.07113*, 2022.

[30] I. Tomar, S. Indu, and N. Pandey, *Traffic Signal Control Methods: Current Status, Challenges, and Emerging Trends*, D. Gupta, Z. Polkowski, A. Khanna, S. Bhattacharyya, and O. Castillo, Eds. Singapore: Springer Nature Singapore, 2022.

[31] N. Geroliminis and J. Sun, "Properties of a well-defined macroscopic fundamental diagram for urban traffic," *Transportation Research Part B: Methodological*, vol. 45, no. 3, pp. 605–617, 2011.

[32] N. Geroliminis, M. Saeedmanesh, and K. A., "A linear formulation for model predictive perimeter traffic control in cities," *Elsevier*, vol. 50, 2017.

[33] "Simulation of Urban Mobility : SUMO," https://sumo.dlr.de/docs/index.html, accessed: 2023-09-11.

[34] "Handbook emissions of emission factors for road transport," https://www.hbefa.net/, accessed: 2024-03-27.

[35] A. Rimoldi, C. Cenedese, A. Padoan, F. Dörfler, and J. Lygeros. (2023) Urban traffic congestion control: a DeePC change.